

A Novel Approach to 3D Laser Scanning

David Wood*, Mark Bishop

Ocular Robotics, Sydney, Australia

{d.wood, m.bishop}@ocularrobotics.com

Abstract

This paper presents a novel 3D laser scanner and compares its performance to that of a range of approaches presently in-use. Each of the alternatives are discussed with respect to a selection of key performance metrics, and the new scanner is also analysed within this context. Examples are then presented where the impact of these performance metrics on real-world applications are illustrated through a simulation, and the new scanner is demonstrated to provide significant advances over existing technologies.

1 Introduction

One of the most ubiquitous tools for modern computer perception is the scanning LiDAR. These tools enable engineers to build two or three dimensional models of the world which can be used for navigation, obstacle detection and avoidance, target tracking or many other applications. For the past decade, researchers have been exploring ways to move beyond the traditional 2-dimensional planar laser scanner and effectively acquire 3-dimensional point clouds. For some applications such as Surmann *et al.* [2001], the goal has been to build structured models of the world, for others [Mertz *et al.*, 2012] the goal is to detect, track and classify objects within the world. Work is also being done at a higher level, on the analysis of generic 3D point cloud data [Douillard *et al.*, 2011]. As autonomous systems gain higher levels of intelligence and the ability to reason on perceived surroundings more effectively, then it becomes desirable to acquire commensurately information rich data on these surroundings. Given the resolution and accuracy limitations of radar and stereo vision based systems, 3D LiDARs remain the sensor of choice for generating such data.

In Section 2, we will discuss a number of such sensors in-use for various applications in robotics. These sensors will be compared with respect to a basic set of performance metrics. In Section 3, we will present our novel

sensor design, the Ocular Robotics RE05. This sensor enables the flexible acquisition of 3D laser data. The sensor can be re-configured on the fly to a significantly wider range of resolution and scan speed behaviours than existing sensor approaches. Section 4 will discuss in detail the performance capabilities of the new scanner. Section 5 then discusses the performance of the RE05 and other sensors from Section 2 with respect to a number of simulated application examples. This section shows the impact of the variation in performance metrics from earlier sections on simulated real-world problems.

2 Comparison With Existing Approaches

In this section, the performance of a number of approaches to 3D LiDAR will be examined. Specific examples of each of the styles of 3D LiDAR have been selected, based on identified applications in robotics. For each of the classes of actuated scanner, we have identified commercially available packages to examine, as these are the best documented in their performance when compared to the homebrew systems developed internally in many robotics laboratories.

2.1 Sensor Categories

The first of these is the actuated 2D laser, where a planar laser scanner is actuated to rotate through a third axis to sweep an area with the scan plane. This has been a very common approach for robotics applications particularly in the past when there were very few other options. Frequently these systems used one or more Sick LMS 2xx devices with the actuating component being fabricated by the end user as seen in [Mertz *et al.*, 2012; Pervolz *et al.*, 2006; Surmann *et al.*, 2001]. The most common configuration is the ‘nodding’ configuration, as illustrated in Figure 1. There are commercially available versions of such systems, such as the Fraunhofer IAS sensors. In this comparison the 3DLS-N and the 3DLS-K2 will be used.

Another common approach are dedicated 3D LiDAR



Figure 1: The Fraunhofer IAS 3DLS-N mounted on a VolksBot (www.volksbot.de).

scanners that use a spinning or nodding mirror to provide one scanning axis and either all or a large proportion of the whole device is then rotated to provide the second scanning axis. In mobile robotics, these sensors are typically used for mapping and surveying rather than online applications due to the time taken to acquire a scan. One example of such an application is shown in Figure 2, the scanning platform as used in [Lim and Suter, 2009]. A similar sensor is the Riegl LMS-Z390i which will be used for the purpose of this comparison.



Figure 2: The scanning platform used in [Lim and Suter, 2009], showing the Riegl LMS-Z420i laser scanner.

The third approach that will be considered here is the spinning array configuration where an array of individual LiDAR sensors is spun about an axis to produce a number of 2D scans at different angles with respect to the spinning axis. This is currently one of the most common approaches, with sensors such as those produced by Velodyne being applied to an extremely wide range of mobile robotics problems [Douillard *et al.*, 2011; Neuhaus *et al.*, 2009; Kammel and Pitzer, 2008]. These

works all use the Velodyne HDL-64E shown in Figure 3 and this is the sensor used in our comparison.

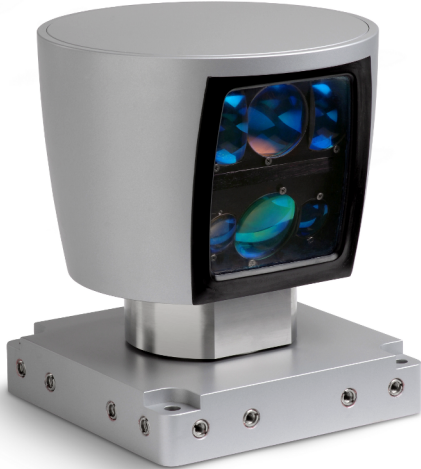


Figure 3: The Velodyne HDL-64E.

2.2 Performance Metrics

For our analysis, we have investigated seven key performance metrics applicable to 3D LiDAR systems:

- *Resolution*: The spatial resolution at which it is possible to gather 3D data determines the level of detail that can be represented by the data.
- *Axis Angular Rates*: Angular rates possible for each axis of scanning.
- *Scan Pattern Flexibility*: The flexibility to focus the attention of a 3D LiDAR scanner to a region of interest and resolution required and update these parameters during operation.
- *Data Rate*: Possible measurement rates of the range finding element.
- *Field of Regard*: The field which can be covered by the LiDAR scanner for all possible mechanical configurations of its scanning mechanism.
- *Size and Weight*: Size and weight often determine a sensors suitability for a particular robotic platform.
- *Cost*: Costs have been ascertained as accurately as possible in Australian dollars.

The application of this set of metrics to the sensors discussed in Section 2.1 is shown in Table 1

	Resolution (Az x El)	Axis Angular Rates (Az x El)	Scan Pattern Flexibility	Data Rate	Field of Regard (Az x El)	Size(mm) Weight (kg)	IP Rating	Cost (AUD)		
Fraunhofer 3DLS-N	0.25° Az	19 Hz Az	El. Rate El. Range Az. Resolution (0.25° – 1.0°)	7.6kHz	100° Az	166mm H	65	\$11,200		
	0.25° El	0.04Hz El			124° El	286mm W				
Notes	1.0° Az	75Hz Az	13.6 kHz	180° Az	166mm D	7.4 kg				
	1.0° El	0.3Hz El			124° El					
Fraunhofer 3DLS-K2	0.25° Az	0.03Hz Az	Az. Rate El. Resolution (0.25° – 1.0°)	15.2kHz	360° Az	320mm H	65	\$20,000		
	0.25° El	19Hz El			200° El	500mm W				
Notes	4.0° Az	1.67Hz Az	27.2 kHz	360° Az	500 mm D	13.0 kg				
	1.0° El	75Hz El			360° El					
Riegl LMS-Z390i	0.001° Az	0.042Hz Az	El. Rate	11kHz	360° Az	463mm H	64	\$200,000		
	0.001° El	20Hz El	Az. Rate El. Range Az. Range		80° El	210mm ø				
Note	The LMS-Z390i allows varying the elevation scan rate between 1Hz and 20Hz in rotating mirror mode and allows adjustment of the elevation range in oscillating mirror mode. Azimuth scan range can be varied between 0° and 360° with azimuth scan rates between 0.00003Hz and 0.042Hz.									
Velodyne HDL-64E	0.09° Az	15Hz Az	Az. Rate	1300 kHz	360° Az	250mm H	67	\$75,000		
	0.4° El	- El			26.8° El	200mm ø				
Note	The HDL-64E allows the azimuth scan rate to be varied between 5Hz and 15Hz. It has no elevation scan capability as it has an array of 64 LiDARs at approximately 0.4° intervals across its 26.8° elevation field.									
Ocular Robotics RE05	0.01° Az	20Hz Az	Full Field	30 kHz	360° Az	300mm H	67	\$22,000		
	0.01° El	3Hz El	Bounded El. Region Scan		70° El	150mm W/D				
Note	Details of the performance and scan patterns are discussed in Section 4									

Table 1: The comparison table for existing commercially available 3D LiDAR systems.

3 RE05 System

This section will discuss the design and implementation of the RE05 laser scanner, as shown in Figure 5. In Section 3.1, we will examine the mechanics of the RE05, and the aspects of the drive mechanism which allow for its unique performance. This is followed by a discussion of the electrical aspects of the system (Section 3.2), focussing on motor control and interfacing. Lastly, Section 3.3 is a brief discussion of the software interface approach, highlighting the flexibility which can be ob-

tained through a relatively simple UDP interface.

3.1 Mechanical Design

The core of the RE05 system is the unique mechanical design of the optical pointing head, shown in Figure 6. There are three main components to this system. Firstly, the laser module itself is a 1D OEM laser range finder. It supports sample rates of up to 10 KHz with intensity returns, and 30 KHz with range-only measurements. Nominal maximum range is 30m to a 10% reflectivity target, and 200m to a retro-reflector. The beam-path for this



Figure 4: The complete RE05 laser scanner. The scan head is mounted inside an IR-pass filter dome (shown cutaway).

1D sensor is directed up the centre of the device into the optical head, and is then re-directed to enable scanning.

The drive unit, as marked on Figure 6 consists of two custom-wound 24V brushless DC motors, capable of rotation rates up to 30 revolutions per second. These motors drive the scan head through a pair of concentric shafts, which means the stators of both motors remain stationary at all times. This is in direct contrast to approaches such as those discussed in [Bergh *et al.*, 2004], where one of the drives must be moved in order to scan the field of view of the sensor. By keeping the motors stationary the mass of the moving parts is greatly reduced, requiring less power, and allowing faster response time, higher precision, and better control. The position of these motors is monitored through a pair of 36000 tick-per-revolution magnetic quadrature encoders.

The scan head itself consists of a number of optical elements. These are connected through the drive-train in a manner to ensure the optical path for the laser is always in through the aperture and down the centre of the device. The core mechanism has two axes of rotation, the θ or azimuth axis, parallel to the axes of the drive shafts, and the ϕ or zenith axis, inclined relative to the

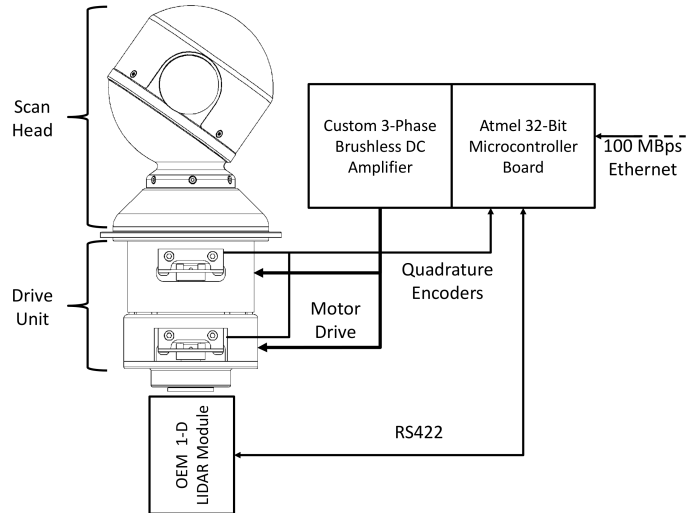


Figure 5: A block diagram of the RE05 laser scanner.

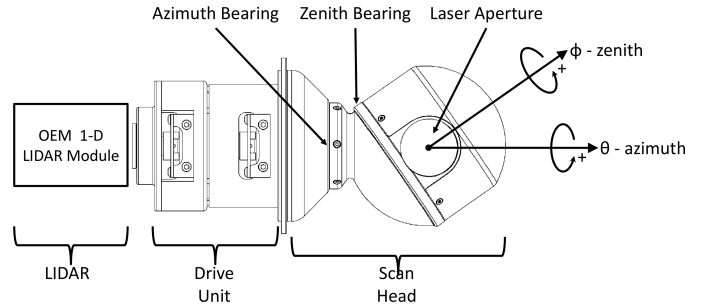


Figure 6: The scanning head assembly of the RE05 sensor, showing the θ and ϕ axes of rotation.

θ axis by 35^0 . This enables the aperture to scan through a full 360^0 in azimuth relative to the body, and $\pm 35^0$ in elevation. This mechanism contains no gearing, and is all directly driven from the drive unit. As a result, there is no backlash present in the scanning head. This lack of backlash ensures that the full 36000-tick encoder resolution is available for locating the head in both θ and ϕ . The scan head is also extremely light, with the moving components massing approximately 140g. This mass is also well balanced around the centre of rotation in both axes. By minimising and balancing the moving mass, scan performance in both θ and ϕ axes is greatly improved over sensors discussed in Section 2.

The RE05 Scan unit is then packaged into an IP67 enclosure, which includes an IR-pass filter dome to minimise the effect of sunlight in outdoor scans.

3.2 Electrical Design

The control and interface of the RE05 is centred around the custom motion control and fusion board shown in Figure 7. This board is based around an Atmel UC3

family 32-bit microcontroller, running at a 66MHz core clock. The UC3 interfaces to the host over a 100MBps Ethernet interface, and to a dual-chip motor control solution on the same board. The UC3 also communicates with the OEM laser ranger over a serial connection and fuses the range readings with synchronised encoder samples to produce range-bearing-elevation observations. These observations are then transmitted over the same 100MBps ethernet interface used for control, giving a single point-of-connection to the RE05.

The motion control solution is a 2-chip Magellan solution produced by PMD. This chip closes a separate PID control loop around each of the axes at a rate of 6.15 kHz. Although the control is independent at this level, higher-level co-ordination is implemented on the UC3 to ensure synchronised behaviour of both axes within the scanner.

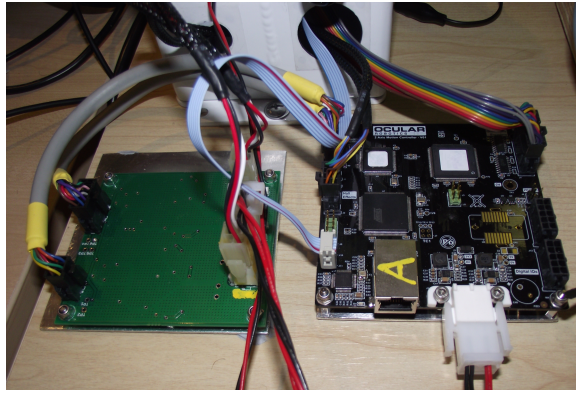


Figure 7: The RE05 control PCBs. Amplifier with its heatsink on left. μ P board on right.

3.3 Software Interface Design

The software interface to the RE05 is based on the UDP protocol to minimise overheads and latency. Ocular Robotics will publish the complete specification of the software interface at a UDP level, enabling systems integrators to work directly with a well-known communications standard and being completely agnostic to the host operating system or computing architecture. The interface is specifically designed to be minimal, there are 3 classes of command with less than 10 commands in each class.

- RobotEye System Commands - These commands enable the presence of RE05's on a network to be detected, and properties such as their IP address and startup behaviour to be configured.
- Laser Management Commands - These commands enable the direct management of the behaviour of the built-in laser module, specifying sample rates, averaging, min and max ranges, and other settings.

- Scan Pattern Commands - These 3 commands enable the properties of a scan pattern to be configured, such as Azimuth rate, line spacing, and the boundaries for bounded-elevation and region scan modes.

From an end-user perspective, the scan patterns mentioned in the last point above highlight the adaptability of the RE05 scan patterns. Figure 8 shows the 3 scan patterns presently implemented on the RE05. The speed with which these patterns can be executed is limited by the velocity and acceleration limits of the scanning head, as discussed in Section 4.

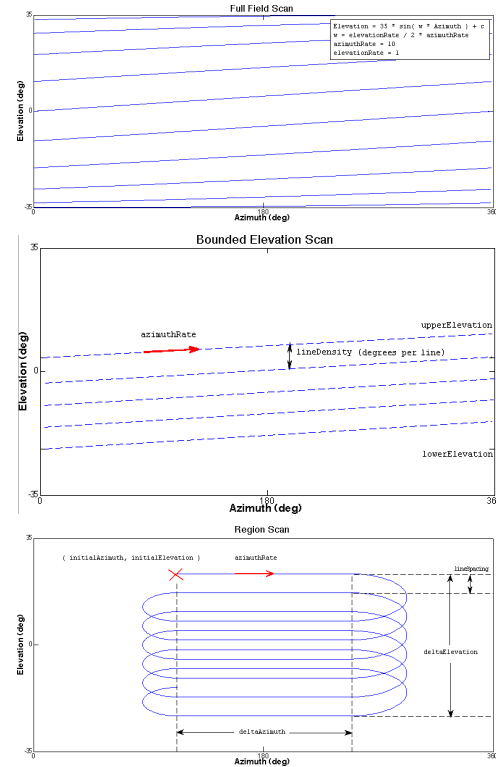


Figure 8: The three scan patterns implemented on the RE05.

4 RE05 Performance

As discussed earlier, there are three main factors at play which provide the scanning performance of the RE05.

- Low moving mass
- Stationary motors and sensor
- Well-balanced moving mass

As all three of these factors have been highly optimised, the RE05 can attain sustained aperture accelerations of up to $100,000^0/\text{sec}$, and can scan with continuous aperture velocities of up to $7,200^0/\text{sec}$.

The eye operates in two distinct scan behaviours. In full-field and bounded elevation scan modes, the eye rotates at a constant azimuth rate whilst scanning in a raster pattern with a specified line resolution. In this behaviour the limit to the performance of the scanner is the maximum allowable velocity. This limit is investigated in more detail in Section 4.1.

The other primary behaviour is piecewise linear motion. This is the behaviour that is used to generate the region scan mode. In this mode, the performance limit is the acceleration of the aperture, and the aperture trajectories are triangular (constant acceleration). This style of trajectory is analysed in detail in Section 4.2.

These two trajectory types also relate to the resolution at which range samples are acquired. The links between this resolution and the scan patterns being performed are discussed in more detail in Section 4.3.

4.1 Velocity Limited Trajectory Performance

The scan rates of the RE05 in full-field and bounded-elevation scan modes are limited by the peak velocity of the scan head itself. The highest-rate motion is the scanning of the entire head around the azimuth axis, slow rotation around the zenith axis then introduces the spiral pattern producing the diagonal line pattern shown in Figure 8. The rate limits for the two axes are $7,200^0/\text{sec}$ for azimuth motion and $540^0/\text{sec}$ for zenith motion. A full-field scan running at these rates would give a line spacing of approximately 10.5^0 per line between $\pm 35^0$ in elevation, and a full field refresh rate of 3Hz.

In bounded elevation scans, this refresh rate could be increased, by maintaining the same elevation resolution and decreasing the region of elevation to be scanned. The limiting case for this is a 2D line-scan pattern, where there is no azimuth motion at all. The scan elevation can be anywhere within the range with no performance penalty. For the line-scan behaviour mode, line rates of 20Hz are possible.

These behaviours can be changed at any time, with the responsiveness of the scan head being limited by the $100,000^0/\text{sec}$ acceleration limit of the scan head. This limit enables the head to transition from stationary to a full-speed scan in approximately 75 mSec, and to transition from full-speed scan to stopped at an arbitrary location within the field of view in 125 mSec.

4.2 Acceleration Limited Trajectory Performance

The scan rate of the eye in region scan mode is limited by the acceleration capability of the scan head. When operating in region scan mode, the head reverses direction at the end of each line, so it's behaviour can be approximated as a sequence of point-to-point motions

where the eye comes close to a stop at each point. Figure 9 shows the performance of the eye in a back-and-forth azimuth scan pattern of 270^0 with 200 millisecond dwells at each point. The noise in the acceleration trace is due to some timing instability in the commercial motor controller used to perform these tests, and a soft tuning of the PID controller. The transition phase of each of these motions is a triangular velocity segment taking approximately 150 mSec.

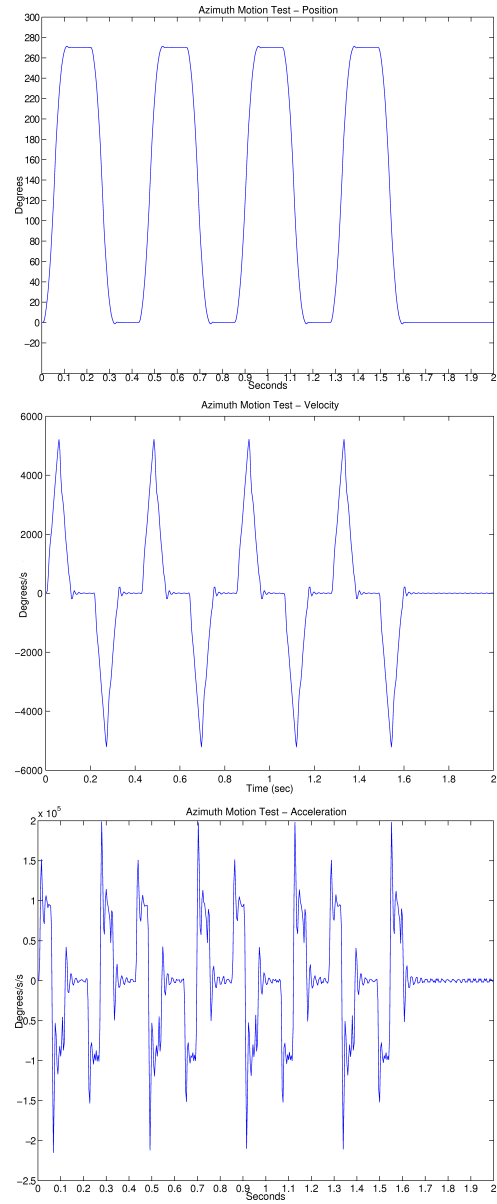


Figure 9: The results of basic azimuth point-to-point motion testing. Note the peak accelerations exceeding $-2 \times 10^5^0/\text{sec}^2$ above sustained accelerations of $1 \times 10^5^0/\text{sec}^2$.

This type of behaviour represents the equivalent to a

region-scan type behaviour. The limiting factor in these motions is the acceleration of the scan head. Under full acceleration, the eye will take 260^0 of motion to achieve peak velocity, requiring a scan pattern line width of 520^0 to reach the velocity limit. We can therefore guarantee that any region scan behaviour will be executed using triangular velocity trajectories, since the region window cannot possibly be wider in azimuth than 360^0 .

Based on triangular trajectories such as these, within a region of angular width d , peak velocity during a line can be calculated as:

$$V_{peak} = \sqrt{2a \times (d/2)} \quad (1)$$

giving a time to execute that line of:

$$T = \frac{d}{V_{peak}/2} = 2\sqrt{\frac{d}{a}} \quad (2)$$

This behaviour is of great benefit when it is desirable to perform an adaptive region scan. As the width of the region to scan grows larger, the time taken to scan the area grows deterministically, linearly in elevation resolution and elevation range and sub-linearly in azimuth range. This enables directed perception systems to make educated decisions regarding the best use of the sensor.

This deterministic relationship also provides an interesting limit. There will be many cases of region scans for which it is more efficient to run the eye in a bounded-elevation scan mode than to decelerate and accelerate at the end of each line. If running at peak velocity of $7,200^0/\text{sec}$, each line scan in full-field or bounded elevation mode takes 50 msec. For an average acceleration of $10^5^0/\text{sec}^2$, this corresponds to a region scan line width of $\frac{0.05^2 \times 10^5}{2} = 125^0$. For any region scans wider than this limit, higher line rates will be achieved by running the eye in bounded elevation mode and segmenting out the region of interest.

4.3 Range Sample Density

The final component of RE05 performance which has not yet been discussed is the relationship between scan density and motion speed. One of the great benefits of the RE05 system is the independence between sampling rate and scan speed. Since the parameters of the 1D laser are managed independently, the sample rate, averaging and information level can all be tailored to the particular scan of interest. The scan resolution in azimuth is determined by a combination of the sample rate and scan speed.

The worst-case scenario for a 30kHz sample rate is to be scanning at $7,200^0/\text{sec}$, which gives an azimuth angular resolution of 0.09^0 . If intensity values are required, the laser sample rate must be reduced to 10 kHz, giving a worst-case resolution of 0.27^0 . Again, the choice of

whether or not to acquire intensity information can be changed at any time, enabling a system to intelligently select between high-frequency data or more informative data based on the task required.

The laser can also perform multiple-sample averaging in hardware. This is only available on the low-rate mode which returns intensities, however when averaging 2 or more samples, the laser will support underlying sample rates up to 15 kHz. This gives an output averaged sample rate of 7.5 kHz or below when averaging in hardware. Where the processing power to do so exists, it will always be more effective and informative to use a kernel-based filter over the high-rate data on a processing host than to average in the laser hardware. For applications where this is not possible, it does provide a simpler option which can result in a reduction in range uncertainty without imposing additional processing burdens on the host.

5 Application-Based Comparison

In this section, the performance of the sensors will all be compared based on a simulated real-world problem. The ability to acquire a 300mm diameter round target somewhere in the sensor's field of regard. The target in question is taken to be 90% reflective, and in order to acquire the target we are specifying that at-least 3 points in azimuth and 3 points in elevation are observed across the target. This gives the minimal detection case as shown in Figure 10.

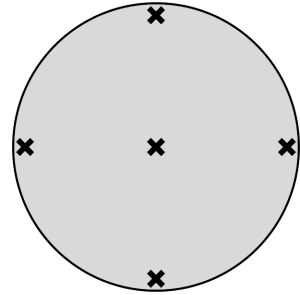


Figure 10: Diagram illustrating the minimum required 5 points on the target to be regarded as a 'detection'.

The three measures used in this section are the range at which the target can be detected, the percentage of the total spatial volume over which the target can be detected, and the time taken for each sensor to scan its field of regard. For all sensors, we first investigate these metrics as taken for a scan of the full field of regard of the sensor, the results for which are presented in Section 5.1. If there is prior information regarding the location of the target, then the 3DLS-N, the LMS-Z390i and the RE05 can all be configured to scan only the region of interest, and Section 5.2 discusses the simulated performance of

these sensors when scanning a more restricted area.

5.1 Full field scans

In these comparisons, each sensor is scanning its full field of regard. For the sensors with tunable resolutions (all bar the Velodyne), it has been assumed that there is a level of prior knowledge about the size of the target, and that the sensor is configured to minimise the time spent scanning without reducing the range at which it is possible to acquire the target.

Sensor	Target Range (m)	Volume Ratio	Scan Time (sec)
3DLS-N	68.7	63.4%	26.1
3DLS-K2	68.7	63.4%	75.79
LMS-Z390i	400	100%	450
HDL-64E	42.9	4.59%	0.066
RE05	200	100%	87.5

Table 2: Results of full-field target detection test. Volume Ratio is the percentage of the full field-of-regard of the sensor over which the target can be seen.

There are a number of interesting results seen in this table. The first is the poor performance of the Velodyne, with its 0.4^0 elevation resolution proving to be a significant obstacle. The 3DLS modules both perform quite well, however they cannot match the detection range given by the RE05 and Riegl systems. Performing a scan adequate to detect such a small target has also proven quite a challenge for these sensors. The long scan times exhibited by the 3DLS-K2, RE05 and Riegl are mostly due to the high-resolution scan requirements limiting the motion speed.

5.2 Limited field scans

Three of the above five sensors allow a level of customisation of the scan pattern. For the 3DLS-N the scan range can be limited in the elevation axis to a smaller region of regard. For the LMS-Z390i, the scan area of both axes can be limited. The publicly available documentation for this module does not specify the line-scan rates the system is capable of in oscillating mirror mode, so we shall assume the Riegl remains in rotating mirror mode with a 20Hz refresh rate. For the RE05, the time taken to scan the region is calculated using Equation 2 and the desired line density.

We assume for this that the position of the target is known to an accuracy of ± 5 times the target diameter, and that we are happy to only partially record the target at short ranges, so the region to be scanned is a square region 10 times the target's apparent size at the maximum detection range identified in Section 5.1.

Again, this section shows interesting results. For the Riegl sensor, the bounded scan was still time-limited by

Sensor	Region Scanned	Scan Time (mS)
3DLS-N	100^0 Az 2.5^0 El	173
LMS-Z390i	0.43^0 Az 80^0 El	560
RE05	0.86^0 Az 0.86^0 El	76

Table 3: Region scan target detection test.

the speed of rotation about the azimuth axis. Even when the region to be scanned is reduced to less than 0.5^0 , the Riegl is still the slowest scanner being studied. The RE05 has demonstrated that the use of the region scan mode in this application results in a substantial time saving, even at the high scan resolutions being produced.

5.3 Discussion

The simulations above in conjunction with Table 1 show that the RE05 fills a vacant niche in the 3D laser scanners presently on offer. It offers a completely unparalleled level of programmability of scan region, with Table 3 showing the substantial improvements in scan times possible by restricting the scan region appropriately. It also offers much greater flexibility of resolution when compared to existing sensors, with the azimuth and elevation resolutions both programmable down to an extremely fine resolution. This flexibility is supported by extremely high dynamic performance due to the mechanical design of the scanning head as discussed in Section 3.1.

The RE05 therefore fills an important niche within the stable of 3D LiDAR sensors currently on the market. The flexibility will offer a previously unavailable opportunity to gather information about adaptable specific regions within a sensor's field of regard. This region-specific information can be gathered at higher resolution and more rapidly than is possible with existing technologies.

6 Conclusions

This paper has presented a novel 3D LiDAR system, the Ocular Robotics RE05. This scanner was benchmarked against a range of existing commercially available scanners, chosen to represent a cross-section of 3D LiDAR solutions. The existing approaches were compared to the RE05 over a range of performance metrics, and were also discussed with respect to a real world problem, detecting a circular target of known size. In this analysis, the flexibility of the RE05 was demonstrated to provide considerable improvements over existing technologies in the acquisition of region scans. The RE05 was also shown

to be unique in its capability to provide high performance whilst being capable of adapting resolution and scan speeds intelligently to the task at hand.

References

- [Bergh *et al.*, 2004] C. Bergh, L. Matthies, and B. Kennedy. A compact and low power two-axis scanning laser rangerfinder for mobile robots. Technical report, DSpace at Jet Propulsion Laboratory [<http://trs-new.jpl.nasa.gov/dspace-oai/request>] (United States), 2004.
- [Douillard *et al.*, 2011] B. Douillard, J. Underwood, N. Kuntz, V. Vlaskine, A. Quadros, P. Morton, and A. Frenkel. On the segmentation of 3d lidar point clouds. In *Proceedings of the 2011 IEEE International Conference on Robotics and Automation (ICRA)*, 2011.
- [Kammel and Pitzer, 2008] S. Kammel and B. Pitzer. Lidar-based lane marker detection and mapping. In *2008 IEEE Intelligent Vehicles Symposium*, 2008.
- [Lim and Suter, 2009] Ee Hui Lim and David Suter. 3d terrestrial lidar classifications with super-voxels and multi-scale conditional random fields. *Computer-Aided Design*, 41(10):701 – 710, 2009.
- [Mertz *et al.*, 2012] Christoph Mertz, Luis E. Navarro-Serment, Robert MacLachlan, Paul Rybski, Aaron Steinfeld, Arne Suppe, Christopher Urmson, Nicolas Vandapel, Martial Hebert, Chuck Thorpe, David Dugins, and Jay Gowdy. Moving object detection with laser scanners. *Journal of Field Robotics*, 2012.
- [Neuhaus *et al.*, 2009] F. Neuhaus, D. Dillenberger, J. Pellenz, and D. Paulus. Terrain drivability analysis in 3d laser range data for autonomous robot navigation in unstructured environments. In *Proceedings of the 2009 IEEE Conference on Emerging Technologies & Factory Automation (ETFA)*, 2009.
- [Pervolz *et al.*, 2006] Kai Pervolz, Hartmut Surmann, and Stefan May. 3d laser scanner for tele-exploration robotic systems. In *Proceedings of the International Workshop on Safety, Security and Rescue Robotics (SRRR)*, August 2006.
- [Surmann *et al.*, 2001] Hartmut Surmann, Kai Lingemann, Andreas Nuchter, and Joachim Hertzberg. A 3d laser range finder for autonomous mobile robots. In *Proceedings of the 32nd International Symposium on Robotics (ISR)*, 2001.